



Geochemical behavior and radiological hazards assessment of phosphorites at the eastern part of the economic phosphate-belt, Egypt.

Sameh H. Negm, Wael M. El Maadway, Amal S. Nasr*

Nuclear Materials Authority, P.O. Box 530, El Maadi, Cairo, Egypt

Corresponding author: (Amal S. Nasr).

Email address: nedaaeldeen@yahoo.com

Nuclear materials authority, P.O. Box 530, ElMaadi, Cairo, Egypt.

Abstract

Twelve typical phosphorite samples were gathered from five phosphorite sites throughout Egypt's eastern economic phosphatic zone (El-hamrawein, El-Mashash, West Nile, Um Hegara, and El-Mashraa locales). The radioactive hazards of the phosphate deposits in these sites were characterized and assessed using chemical and radiometric investigations. Despite the exception of the west Nile location, where the phosphorite is thought to be of intermediate grade, the chemical examination showed that all the locales have high-grade phosphorite. Additionally, carbonate fluorapatite was the primary mineralogical element in all of the examined phosphorites. The West Nile phosphorite had the lowest uranium level (ppm), according to the radiometric results, whereas El-Mashash phosphorite had the highest. Utilizing a NaI(Tl) detector, rock samples were examined to determine the radiological risks and compare them to worldwide average values. The concentration of activity (Bq/kg) of both ^{238}U and ^{226}Ra recorded much significantly larger values than the averages for the world where the averages of the activity concentration of ^{238}U for all the studied localities ranged between 494 and 1494.4 Bq/kg vs. 33 Bq/kg as the world average, while this value for ^{226}Ra ranged between 177.6 and 1298.7 Bq/kg vs. 32 Bq/kg as the world average. Several radioactive hazard indices were calculated and compared with their corresponding world safe limits where many of them revealed much higher values than the recommended safe limits which mean a high probability for imposing health risks upon the workers into these localities.

Keywords: Phosphate, Geochemical behavior, radiological hazards assessment, annual effective dose Egypt.

Received 25 Jan., 2023; Revised 07 Feb., 2023; Accepted 09 Feb., 2023 © The author(s) 2023.

Published with open access at www.questjournals.org

I. Introduction.

Phosphate ores (phosphorites) are the back-bone raw material for many important industries such as; phosphatic fertilizers, phosphoric acid, cleaners, soaps, detergents and insecticides, in addition to some food processing applications and water treatment. Moreover, the phosphorites are traditionally hosting several strategic elements especially uranium, REEs, thorium and fluorides.

Due to its contents from ^{238}U , ^{232}Th and their decay products also was the ^{40}K , the rock of phosphate is considered as Naturally Occurring Radioactive Material. From the radioactivity point of view, the phosphate rocks include about 1500 Bq/kg (in average) resulted from the activity of its radionuclides content and occasionally up to about 20,000 Bq/kg (Asaduzzaman et. al., 2015, Paschoa et. al., 2002 and El Zrelli et. al., 2019).

The serious issue that relates to manufacturing of phosphoric acid from the phosphorites by the wet method as well as the subsequent production of phosphatic fertilizers is the transportation of most radionuclides content into the products, where about 80% of Ra-226, 30% of Th-232, and 5% of U-238 move into the phosphogypsum (a by-product during phosphoric acid manufacturing). While the uranium content of the fertilizers increases by up to 150% in comparison to the phosphate ore (UNSCEAR, 2008 and Farhan et. al., 2021). Additionally, Phosphate processing might produce gaseous and particle emissions. containing ^{238}U and ^{226}Ra , this may put the public at risk of radiation exposure.

Referring to the Egyptian phosphorite, its reserves were estimated to exceed 3 billion metric tons

(Notholt, 1985) distributed on three East-West trending phosphatic belts (Fig 1) contain approximately 80,000 tons of uranium. These belts from North to South as (Hermina, 1972):

- 1- The most northern belt which extends from Sinai to Bahariya Oasis as thin layers and intercalated by carbonate and sand facies, so it has no economic potentialities-
- 2- The central belt which is considered the almost economic that occurrences and occupies the subsequent localities:
 - a- The land stretch along the Red Sea from Safaga to Quseir.
 - b- The Nile Valley, from Idfu to Qena.
 - c- The Western Desert on Abu Tartur Plateau.
- 3- The third and southern belt have been extended through Aswan and characterized by the association of iron ore accumulations among shallow water sediments. Also, it didn't has economic importance.

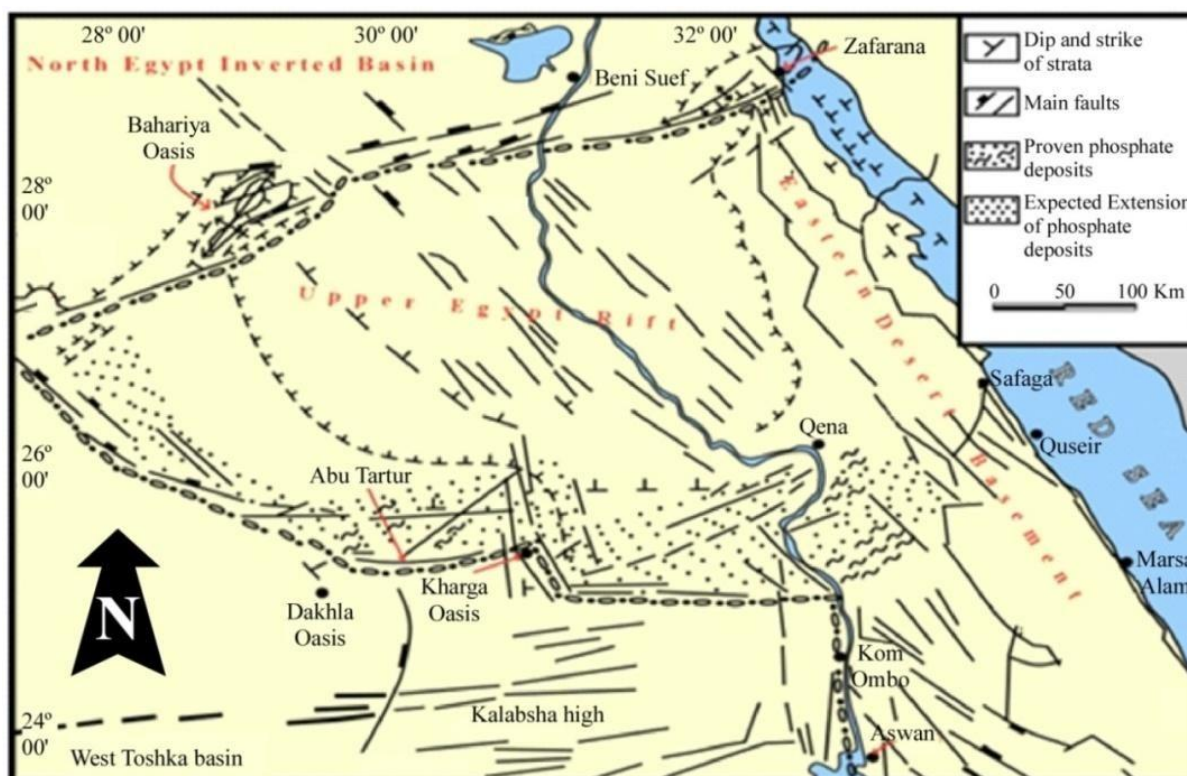


Fig. 1 Phosphate deposits distribution in Egypt(after Khalil and Denchi, 2000).

This study's primary goal is to evaluate the radionuclides' activity concentration U-238, Ra-226, Th-232, and ^{40}K in some Egyptian phosphate rocks and evaluate their potential radiation hazards via computing the radiological hazard indices. Samples from five phosphatic locations within the central belt were the matter of this study and the acquired data were compared against the international recommended safe limit of the radiation hazard to assess the radiological risks that these substances provide to the employees throughout the mining procedures

II. Geological background

Egyptian phosphate belongs to the phosphogenic province which extends along the Middle East-North Africa- Northern South America of the Tethyan Upper Cretaceous to Paleogene (Early Tertiary) age. The Duwi Formation, which contains the phosphorite-bearing series, and its lateral analogues, are thin, widely dispersed, shallow marine deposits that are found in an east-west trending strip that spans Egypt's lower middle latitudes (Germann et. al., 1987).

The Middle-Companion Qusseir Formation's river shale sequence is overlain by the Duwi Formation, which itself is overlain by the Middle-Maestrichtian Dakhla Formation's deeper marine shale and marl sequence. Thus, the Duwi Formation deposition is represent an initial stage of the Late Cretaceous marine transgression in Egypt though its precise age is poorly known, and commonly regarded as being from Late Companion to Early Maestrichtian (Glenn and Arthur, 1990).

The Duwi Formation delineated into phosphorites and phosphatic beds intercalated with various lithofacies, including shales, marls, limestones, cherts, and oyster-rich limestones, and it represents the

establishment of the first fully marine condition. This condition spread across Egypt during the major transgression in the Late Cretaceous.

The studied phosphate samples had been collected from five localities all along with the eastern part of the central economic belt (Fig 2), and the collection process took in consideration any variation could be observed along the phosphorite layer in each locality so, the investigated samples are considered as representative samples for the phosphate rock in each studied locality.



Fig. 2 Location map showing the studied areas and the samples location.

III. Materials And Methods.

3.1. Sample preparation and characterization

Twelve bulk samples were taken from the studied localities (Table 1). All the samples were completely disaggregated to the free particles and then each sample was carefully homogenized and quartered to conduct about one kilogram from each sample to be utilized later in the chemical and radiometric investigations. The quartered samples had been divided into the two parts; one part was mechanically ground to less than 200 mesh sizes for the chemical analysis purpose, while the other part was lightly ground to 100 mesh size for the radiometric investigation process.

Table 1. Number of collected samples from each studied locality.

Locality	Number of representative samples
El-Hamrawein	2
El-Mashash	2
Um Hegara	3
El-Mashroaa	3
West Nile	2

Instrumentation and calibration.

Chemically, the major components of the phosphatic samples were determined and measured using different techniques (based on the measured component include the colorimetric measurement by the UNICAM spectrophotometer (P_2O_5 , SiO_2 , Fe_2O_3 , Al_2O_3), the flame photometric measurement using JENWAY flame

photometer (Na₂O and K₂O), SCHOTT titrimetric technique using EDTA (CaO and MgO) and the ion-selective electrode (F). On the other hand, the trace elements had been identified and measured by using the non-destructive X-ray fluorescence technique (PHILIPS Unique-II spectrometer equipment with an automatic sample changer PW 1510, (30 positions) that had been connected to the computer of the system by using X-40 program for spectrometry.

Measurements of radioactivity.

Preparation of samples.

The rock of phosphate samples had been crushed mechanically into a powdered form, then dried and then ground to have 100 mesh size. These 12 homogenized samples each of which had been weighing 200 g and then were then packed into a containers of polyethylene circular (Merinelli beakers) of 10 cm in diameter and the height is 3 cm. Each sample had been pressed manually in its container till it had been filled and then it is tightly closed and stored sealed for one month to reach the state of equilibrium between radium and their decay product, which is responsible for 98.5% of the radiological impact of the uranium decay products, Uranium and radium's progenitors are typically disregarded for their contributions. As a result, radium rather than uranium is typically used in references to radionuclides from the uranium series (Farai et al. 2005). These studies were performed in the laboratories of the Egyptian Nuclear Materials Authority. Uranium, thorium, radium, and potassium concentrations had been measured by using a high efficiency multi-channel analyzer of gamma-ray spectrometry with a NaI(Tl) detector.

Gamma-ray spectrometry.

Instrumentation and calibration.

The NaI(Tl) gamma ray spectrometer had been used to detect the activity concentrations of Ra-226, Th-232, U-238 and K-40. This is composed of a 76 mm by 76 mm NaI(Tl) crystal Bicron scintillation detector, that is hermetically sealed with the photomultiplier tube of aluminum chassis, that was determined for the sample material. Following that the detector was then insulated from induced X-rays and a lead bricks chamber from radiation of the environment by using shielding of copper cylindrical (thickness, 0.6 cm) and after that the lead sheet was used to seal the detector (thickened 5 cm). Then the detector had been coupled to a main shaping amplifier of Nuclear Enterprises, a model NE-4658, and a high voltage Tennelec of power supply, model TC 952 with a digital display HV. The detector had been coupled to a computer-based Nuclease PCA-8000, 8192 multichannel analyzer with color graphical spectrum display and an advanced operational capabilities. For 86,400 seconds, every sample and the background data had been registered. Then to determine an activity of U-238, Th-232, Ra-226 and K-40, gamma spectroscopy was performed. To ensure that the equipment correctly detects the radioactive elements' gamma radiation energy, using radioactive calibration sources, permanent calibration was performed; ¹³⁷Cs (661.6 keV) and ⁵⁷Co (122.1 keV). By measuring the activity concentration of ²¹⁴Pb, the ²²⁶Ra concentration had been calculated that measured from its 351.9 keV γ -peak, The activity of ²²⁸Ac, as measured by its 911.1 keV peak, that had been used to determine the concentration of Th-232, and the 1460 keV rays, that released by the decay of K-40 itself had been used to assess the concentration of K-40. In the analyzed samples, the radioactivity of natural radionuclides such as U-238 and Th-232 series, as the same as K-40, that was examined. The following formula had been used to determine these radionuclides' radioactivity concentrations (Farai et al., 2005):

$$A \left(\frac{\text{Bq}}{\text{kg}} \right) = \frac{C}{Pwt \epsilon} \quad (1)$$

where **A** is the concentration of activity in Bq/kg, **C** is a net count, that more than a background, **P** is an absolute emission probability of gamma ray emission, **w** is a net weight of dry sample (kg), **t** is the time of measurement, and (**ϵ**) is an absolute efficiency of the detector. The obtained results had been statically analyzed and an uncertainty (**σ**), standard deviation (**SD**), and a standard error (**SM**), had been evaluated at a confidence intervals of 95% (Loucks et al., 2017).

Evaluation the radiological hazards.

In order to evaluate radiological hazards and determine the public radiation risk, many radiological hazard parameters were determined. This variable, including **Ra_{eq}**, radium equivalent content, **D_{air}**, absorbed dose rate, external and internal hazard indices, **AGDE**, annual gonadal dose equivalent and **ELCR**, excess lifetime cancer.

Radium equivalent activity (Ra_{eq}).

The radium equivalent content had been expressed as a radioactive index, that it was evaluated the radiation health risks. Radium equivalent value must not be more than 370 Bq/kg to keep the annual effective dose equivalent of public's lower than 1 mSv. The radium equivalent could be articulated by using the following relation (Ravisankar et al., 2012).

$$Ra_{eq} = A_{Ra} + 1.43A_{Th} + 0.077A_K \quad (2)$$

The abbreviations A_{Ra} , A_{Th} , and A_K stand for the concentrations of activity for ^{238}U , ^{232}Th , and ^{40}K , respectively. The concentrations of activity for ^{238}U , ^{232}Th and ^{40}K , are 10, 7, and 130 Bq/ kg that compare to the identical annual effective dose equivalent of 370 Bq /kg (UNSCEAR, 2000 and NEA-OECD, 1979).

External hazard index (H_{ex}).

The external exposure risk as a result of gamma ray radiation is considered by the external hazard index and obtained by the following equation (Hazou and Patchali, 2021):

$$H_{ex} = \frac{A_{Ra}}{370} + \frac{A_{Th}}{259} + \frac{A_K}{4180} \leq 1 \quad (3)$$

The concentrations of activity for Ra-226, Th-232, and K-40 is denoted by A_{Ra} , A_{Th} and A_K respectively.

Internal hazard index (H_{in}).

The internal exposure of radon gas and its decay products has a risk impact on the respiratory systems, the internal danger index H_{in} is a best indicator of the risk from exposure to radon gas and its decay products.

The internal hazard index H_{in} which is defined as (Khandaker et. al., 2018):

$$H_{in} = \frac{A_{Ra}}{185} + \frac{A_{Th}}{295} + \frac{A_K}{4810} \leq 1 \quad (4)$$

So the maximum radium concentration is half that of the normally acceptable limit, the H_{in} will be ≤ 1 . (Abdullah, 2010).

The representative Gamma Index (I_γ).

(I_γ) be the representative level index for measuring gamma radiation in soil associated with the natural radionuclide. (I_γ) is defined by using following equation (Ebaid et. al., 2012).

$$I_\gamma = \frac{A_{Ra}}{150} + \frac{A_{Th}}{100} + \frac{A_K}{1500} \leq 1 \quad (5)$$

the gamma radiation of hazards is related to the natural radionuclides, that is articulated by the gamma index activity concentration (I_γ). As (I_γ) exceed unity it may cause radiation risk to human (Abo-Elmagd et. al., 2010).

Outdoor radiation exposure.

• External exposure.

The determination of the absorbed dose rate and effective doses is dependent on gamma ray exposure from terrestrial radionuclides in eastern part of Egypt. The outdoor external exposure, that originates from terrestrial radionuclides, which are found in trace amounts in all soils. The higher radiation levels are correlated to the igneous rocks, like granite, and lower levels are associated by sedimentary rocks. However, certain shales and phosphate rocks have rather significant radioactive concentrations.

a. Absorbed dose rate in air (ADRA).

The absorbed dose rate in air according to radiation of gamma has been estimated at 1 m over the ground terrestrial surface. Accordingly all spectrometric measures, the three constituents of radionuclides that emit externally in the U-238, Th-232, and K-40 series contribute almost equally. Individuals should be exposed to the same amount of externally incident gamma radiation whether indoors and outdoors. The factors of conversion used for calculations are 0.462 nGy/h for ^{238}U , 0.604 nGy/hr for ^{232}Th , and 0.0417 nGy/hr for ^{40}K . As a consequence, the absorbed dosage rate may be computed. as following (UNSCEAR, 2008).

$$ADRA \text{ (nGy/h)} = 0.462A_U + 0.604A_{Th} + 0.0417A_K \quad (6)$$

since; A_U ; A_{Th} and A_K are the activities of U-238, Th-232 and K-40, respectively, in Bq/kg.

b. The outdoor effective dose rate equivalent (EDRE_{outdoor}).

The effective dose equivalent rate has been computed by use 0.7 Sv /Gy for the conversion factor coefficient from an absorbed dose rate in air to the adults' effective dose received according to (UNSCEAR, 1993). Then, the outdoor effective dose equivalent rate ($\mu\text{Sv/h}$) according to terrestrial radionuclides ^{238}U , ^{232}Th and ^{40}K at all samples are obtained from the following equation (UNSCEAR, 1993):

$$EDRE_{outdoor} \text{ (}\mu\text{Sv/h)} = ADRA \text{ (nGy/h)} \times 0.7 \text{ (Sv/Gy)} \times 10^{-3} \quad (7)$$

c. The annual effective dose equivalent external (AEDE_{Ex}).

In this study, suppose that the occupational work outdoors all through a studied area for 10 hours per day. Then the outdoor factor occupancy has been corrected to be 0.36. And so, the annual external effective dose equivalent (mSv/y), that received by workers at every location over a studied area is known by (Abdel-Razek et. al., 2016):

$$AEDE_{Ex} \text{ (mSv/y)} = EDRE_{outdoor} \text{ (}\mu\text{Sv/h)} \times 8760 \text{ (h/y)} \times 0.36 \times 10^{-3} \quad (8)$$

Excess lifetime cancer risk (ELCR).

The excess lifetime cancer risk is known as the likelihood of developing cancer throughout a lifetime at a specific exposure level. It was estimated based on the annual effective dose equivalent AEDE_{Ex}, by using the following equation (Ghanim et. al., 2019):

$$ELCR \text{ (mSv/y)} = AEDE_{Ex} \times Dw \times RF \quad (9)$$

Then $AEDE_{Ex}$ is an annual effective dose equivalent external (mSv/y). D_w is a work duration (40-year), and RF (Sv^{-1}) is the coefficient of risk factor, the non-fatal and fatal risks cancer per Sievert. For stochastic effects following low dose rate radiation exposure, ICRP 103 uses values of 0.041 for the adult working individual (ICRP, 2007). Excess lifetime cancer risk refers the increased likelihood of cancer development at the lifetime at the case of exposed humans to the level of radiation.

Annual Gonadal Equivalent Dose (AGED).

The gonads, is an active bone marrow and a bone surface cells, that are considered highly to be the organs of roughly interest with agreement to (UNSCEAR, 2000) as their sensitivity of radiation. The annual gonadal dose equivalent according to of Ra-226, Th-232 and K-40 had been calculated by using the following equation (Abo-Elmagdet et al., 2010 and Arafa, 2004).

$$AGED (\mu Sv/y) = 3.09 C_{Ra} + 4.18 C_{Th} + 0.314 C_K < 300000 \quad (10)$$

The averages world of AGDE of a house, that containing activity concentrations of Ra-226, Th-232 and K-40 are 35, 35 and 370 Bq/kg, respectively. AGED's standard UNSCEAR value is 300 mSv/ y.

Alpha index (I_a).

The maximum recommended level of exposure to Ra-226 is 200 (Bq/kg) and an excess alpha radiation may be computed as (Msilax et al., 2016).

$$I_a = \frac{A_{Ra}}{200} \quad (11)$$

IV. The Results and Discussion.

Chemical composition.

The chemical analysis resultants of an investigated samples (Tables 2&3, Fig. 3) showed the traditional chemical composition of phosphatic rocks with no anomaly signs. However, some remarks could be observed and concluded such as;

1. The west Nile phosphate shows (in average) the lowest P_2O_5 and CaO and the highest MgO contents which means lower phosphate quality than the other areas.
2. Based on the P_2O_5 ratio and according to the classification of phosphorite as function for the P_2O_5 contents (Isil et al., 2010, Negm, 2014 and Esmat A. Abou El-Anwar et al., 2017) it could be concluded that all the studied phosphate are considered high-grade ores (26–35% P_2O_5) except the phosphorite of the west Nile which could be classified as intermediate-grade ore (17–25% P_2O_5).
3. Referring to the fluorine content which exceeds 1% in all the investigated samples it can be concluded that the carbonate fluoroapatite represents the main mineralogical component of these phosphorites (Eduardo Ferreira da Silva et al., 2010) and this conclusion is supported by the average of CaO/ P_2O_5 ratio of the studied phosphate (≈ 1.5) which is in compatibility with the same normative ratio in the carbonate fluorapatite (1.58).
4. The low averages of Al_2O_3 , Fe_2O_3 and MgO (1.2%, 3.0% and 2.6%; respectively) shows that the examined phosphates were precipitated in sedimentary basins.
5. The high silica contented average (11.0%) is a good indicator for the biogenic origin of these phosphates (Germann et al., 1987).

However, the concentrations of the trace elements in a studied samples were generally sourced from the detrital minerals, that were introduced into the rocks by weathering, accompanied with the organic matter or those elements incorporated in the carbonate fluoroapatite crystal lattice (El-Kammar et al., 1979).

Table 2. Major oxides concentrations (%) of a studied phosphate samples.

Locality	S.NO.	P ₂ O ₅	CaO	MgO	SiO ₂	Fe ₂ O ₃	F	Al ₂ O ₃	Na ₂ O	K ₂ O	L.O.I	Total
Hamrawen	H1	29	42.5	2.6	9	3	3	1.4	1.2	0.1	8	99.8
	H2	24	36	5.5	13.5	5.5	2.4	2	1.6	0.2	9.6	100.3
El-Mashash	M3	25	39	5.3	9.2	4.8	1.9	2	1.1	0.2	9.7	98.2
	M4	30	39	4	11	3	2.1	1.5	1.2	0.1	11	102.9
Um Hegara	Um5	27	39	3.3	11	5.1	1.3	1.4	1	0.2	9	98.3
	Um6	30	39.4	3.9	10.3	5	2.1	1.7	1.1	0.4	8.6	102.5
	Um7	25	37.3	3.7	11.5	5.2	2.3	1.9	1.3	0.2	10	98.4
El-Mashroaa	E8	24	35	5.4	13	5	2.2	1.8	1.2	0.1	10	97.7
	E9	28	41	4	10	4	1.5	1.2	1.2	0.2	10	101.1
	E10	30	40	2.7	9	3	2.4	1.6	1.1	0.2	11	101
West Nile	W11	25	39	7	10.9	4.9	1.5	2	1.1	0.3	8.91	100.61
	W12	21	33.6	7.5	13.5	5.2	1	1.8	1.6	0.2	13.7	99.1

Table 3. Trace elements concentrations (ppm) of a studied phosphate samples.

Locality	S.NO.	Cd	Cr	Cu	Ni	Zn
Hamrawen	H1	7	138	24	26	27
	H2	8	97	26	43	155
El-Mashash	M3	25	39	5.3	9.2	4.8
	M4	6	143	27	44	13
Um Hegara	Um5	4	135	11	12	168
	Um6	21	155	31	48	97
	Um7	17	85	20	41	95
El-Mashroaa	E8	8	155	26	42	158
	E9	17	125	11	12	130
	E10	12	139	14	30	95
West Nile	W11	11	115	28	45	205
	W12	7.6	152	24	41	157

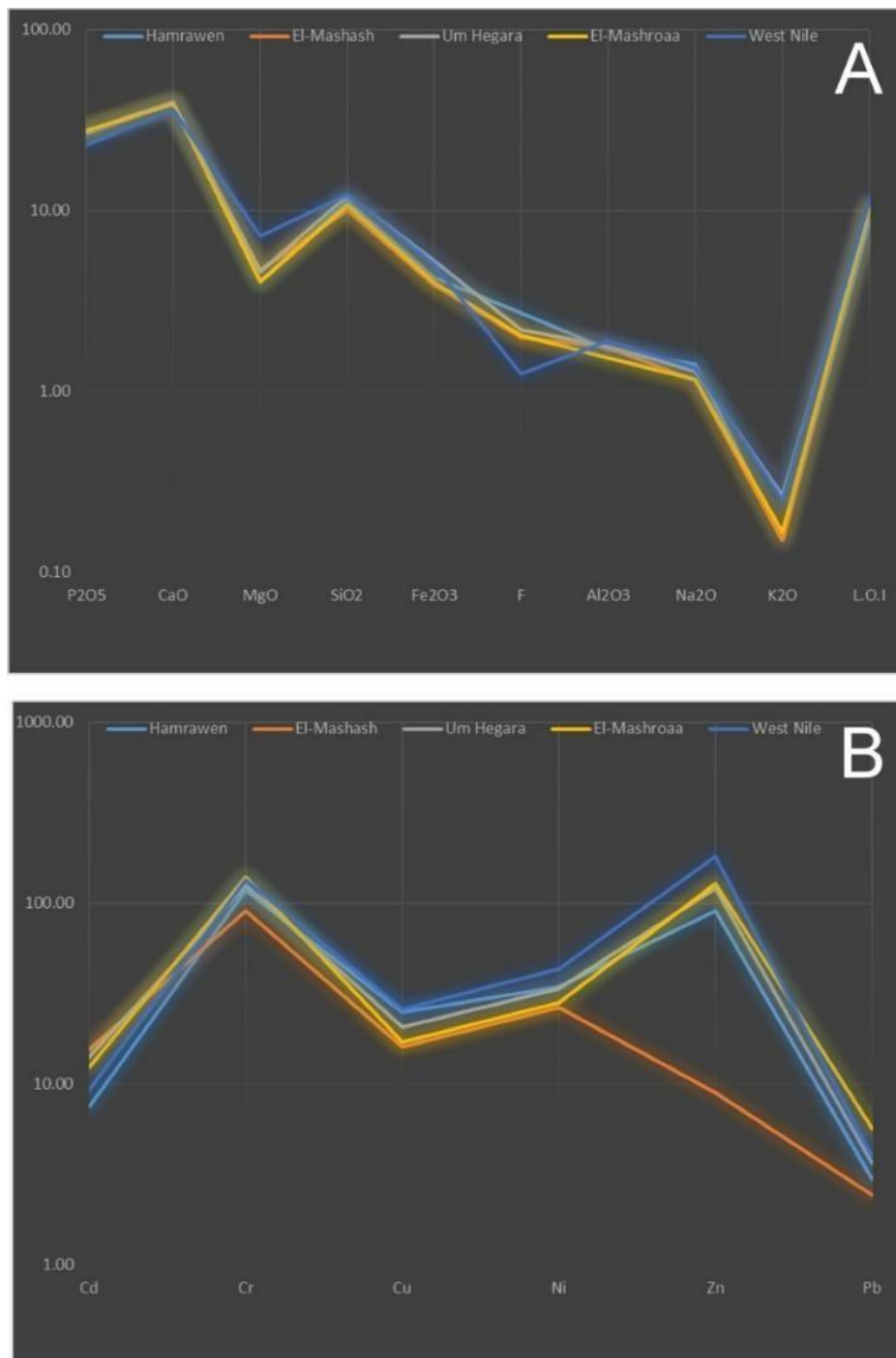


Fig.3 Comparing an average concentration of a major (A) and the trace elements (B) in a studied localities.

Radiological hazards interpretation.

The radiometric assessment of the radionuclides chemical concentration in the studied phosphorites (Table 4) revealed that the highest averages of ²³⁸U and ²²⁶Ra were recorded in El-Mashash locality while the lowest ones are belonging to the west Nile locality, and generally all the localities were affected by uranium enrichment after the deposition process as indicated from the ratios of eTh/eU and eU/eTh.

The specific activity concentrations (Bq/kg) of each sample was computed in (Table. 5) with accordance to the following relations: Potassium1% = 313.00 (Bq/ kg); Uranium1 (ppm) = 12.35 Bq/ kg and Thorium1 (ppm) = 4.06 Bq/ kg, Radium1 (ppm) = 11.10 Bq/ kg (IAEA,2003).

Table 4. The chemical concentrations of ^{238}U , ^{232}Th , ^{226}Ra (ppm) and ^{40}K (%) and some calculated ratios in the studied phosphorites.

Locality	S.NO.	^{238}U (ppm)	^{226}Ra (ppm)	^{232}Th (ppm)	^{40}K %	eTh/eU	eU/eTh
Hamrawen	H1	81	75	3	0.75	0.04	27
	H2	60	68.5	1	0.84	0.02	60
	average	70.5	71.75	2	0.795	0.03	43.5
El-Mashash	M3	66	89	4	0.48	0.06	16.5
	M4	121	117	3	0.36	0.02	40.33
	average	93.5	103	3.5	0.42	0.04	28.42
Um Hegara	Um5	73	91	0.9	1.48	0.012	81.11
	Um6	101	107	0.6	0.6	0.01	168.33
	Um7	83	85	0.6	0.72	0.01	138.33
	average	86.20	95.00	0.7	0.93	0.008	123.14
El-Mashroaa	E8	77	73	4	0.44	0.05	19.25
	E9	85	75	1	0.71	0.01	85.00
	E10	82	83	1	0.76	0.01	82.00
	average	81.20	77.40	2.20	0.62	0.03	58.10
West Nile	W11	47	51	8	1.19	0.17	5.88
	W12	40	46	3	0.92	0.08	13.33
	average	43.50	48.50	5.50	1.06	0.12	9.60

From Table (5), fig. (4) Represent the difference between the activity concentrations of radionuclides in phosphate deposits samples. The U-238 was ranged from (537.2 E to 1154.7 M) Bq/kg with an average of 942.7 Bq/kg then average was more than worldwide limit 33 Bq/kg. In addition to ^{226}Ra was ranged from (399.6 E – 1143.3 M) Bq/kg, and the average was 865.3 Bq/kg that was more than a worldwide limit 32 Bq/kg. Beside ^{232}Th was range from (2.9 Um – 22.3 E), and the average was (10.2 Bq/kg) that less than the worldwide limit 45 Bq/kg. Moreover ^{40}K was ranged from (131.5 M - 330.2 E) and the average was 241.3 Bq/kg that less than the worldwide limit 412 Bq/kg.

From the calculated activity concentrations it is clear that the values of ^{238}U and ^{226}Ra are much greater than the corresponding values according to the world average 14. (UNSCEAR 2000) while those values of ^{232}Th and ^{40}K are lesser than a world average. This contradiction between the high values of ^{238}U and ^{226}Ra from one side and the low values of Th-232 and K-40 on the other side can be understood into the light of decay relation between all these radionuclides where always there is a proportional relation between the existence of ^{238}U and ^{226}Ra , in addition to the mobilization capability of ^{238}U in opposite to ^{232}Th which is known as immobile radionuclide (Figures 5-7).

Table 5. The specific activity of concentrations (Bq/kg) of the radionuclide in the studied phosphorites

Locality	S.NO.	²³⁸ U(Bq/kg)	²²⁶ Ra(Bq/kg)	²³² Th (Bq/kg)	⁴⁰ K(Bq/kg)
Hamrawen	H1	1000.4	832.5	12.2	234.8
	H2	741.0	760.4	4.1	262.9
	average	870.7	796.4	8.1	248.8
El-Mashash	M3	815.1	987.9	16.2	150.2
	M4	1494.4	1298.7	12.2	112.7
	average	1154.7	1143.3	14.2	131.5
Um Hegara	Um5	901.6	1010.1	3.7	463.2
	Um6	1247.4	1187.7	2.4	187.8
	Um7	1025.1	943.5	2.4	225.4
	average	1058.0	1047.1	2.9	292.1
El-Mashroaa	E8	951.0	810.3	16.2	137.7
	E9	1049.8	832.5	4.1	222.2
	E10	1012.7	921.3	4.1	237.9
	average	1004.5	854.7	8.1	199.3
West Nile	W11	580.5	621.6	32.5	372.5
	W12	494.0	177.6	12.2	288.0
	average	537.2	399.6	22.3	330.2
max		1154.7	1143.3	22.3	330.2
min		537.2	399.6	2.9	131.5
Total average		942.7	865.3	10.2	241.3
Worldwide average [14]		33	32	45	412

Table (6) illustrates the radiological hazard parameters' mean, lowest, and maximum values; Radium equivalent (Bq/kg), External and Internal Hazard Indices Representative gamma index, absorbed dose rate in air, External effective dose rate equivalent outdoor, annual effective dose equivalent external, excess life cancer, and Alpha index, Annual gonadal dose equivalent, for all phosphate rock samples.

Table (6) show that, the radium equivalent (R_{eq}) extend from 457 W to 1173.7 M (Bq/kg) with an average of 898.5 Bq/kg, that is larger than a recommended limit of 370 Bq/kg, that keeps the external dose lower than 1mSv/y (Ravisankar et. al., 2012). The hazard indices, (H_{ex}) and (H_{in}) of the examined values exhibited in table (6), figure (8). the external hazard index (H_{ex}), can be depict that samples were on the range of 1.2 W - 3.2 M, with average 2.4. Those values higher than threshold that recommended by (UNSCEAR, 2000) that was ≤ 1 . And that the index hazard of internal radiation (H_{in}) of all the samples was average between 2.3 W - 6.3 M value. with average 4.8. The highest value belonged to M that was 6.3 while the smallest was 2.3 which showed by W sample. This indicates that all sample was higher than unity threshold which recommended by (UNSCEAR, 2000) that was ≤ 1 . Representative level gamma index ($I_{\gamma x}$) According to Table (6) show that the values range between 3.1W - 7.9 M with average 6.1 the highest value was in M while the lowest value showed by W sample. All samples exhibit that the value of ($I_{\gamma x}$) is further more than unity (world limit).

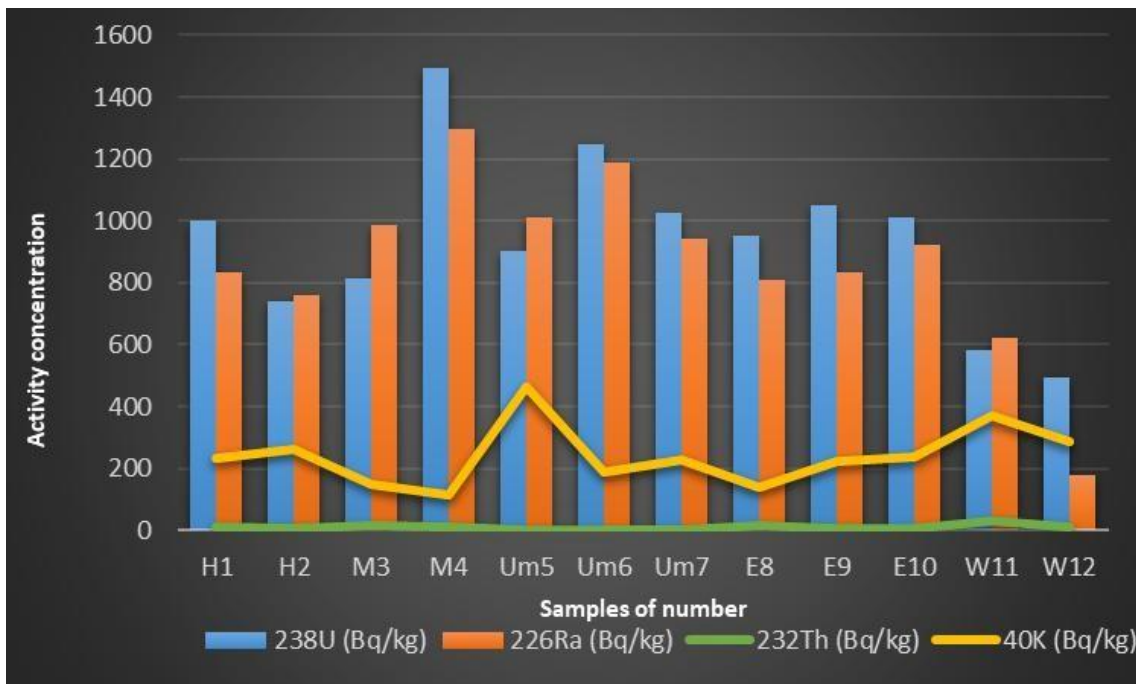


Fig.4 Activity concentration of radionuclides from phosphate ore.

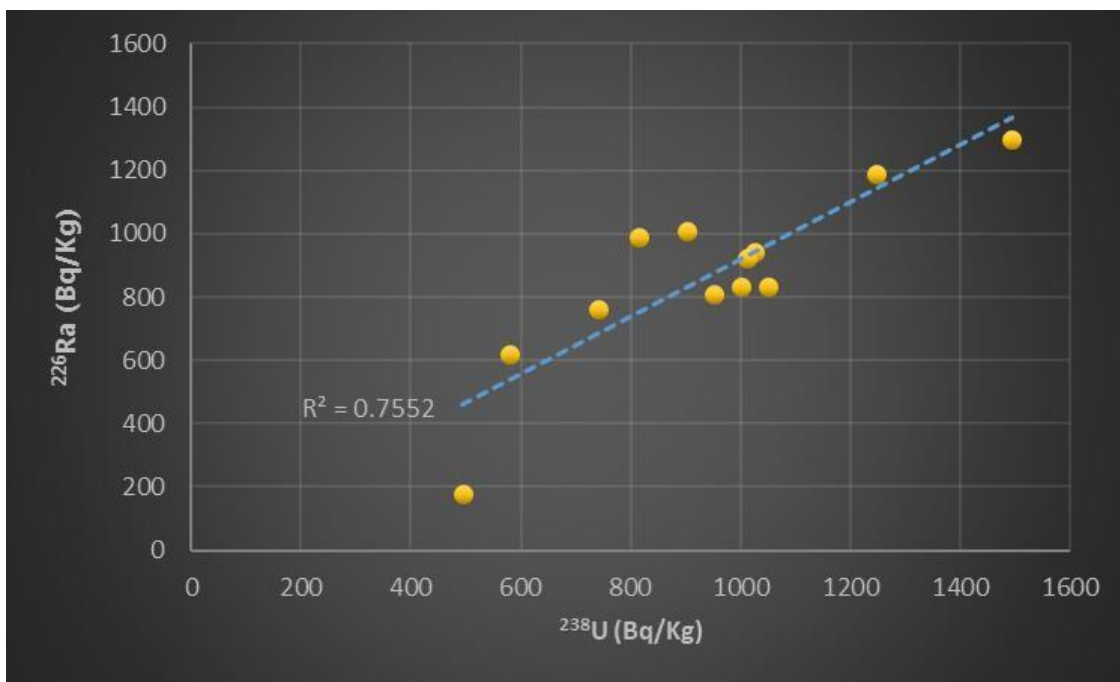


Fig.5 The Correlation investigation between uranium concentration and radium activity concentration.

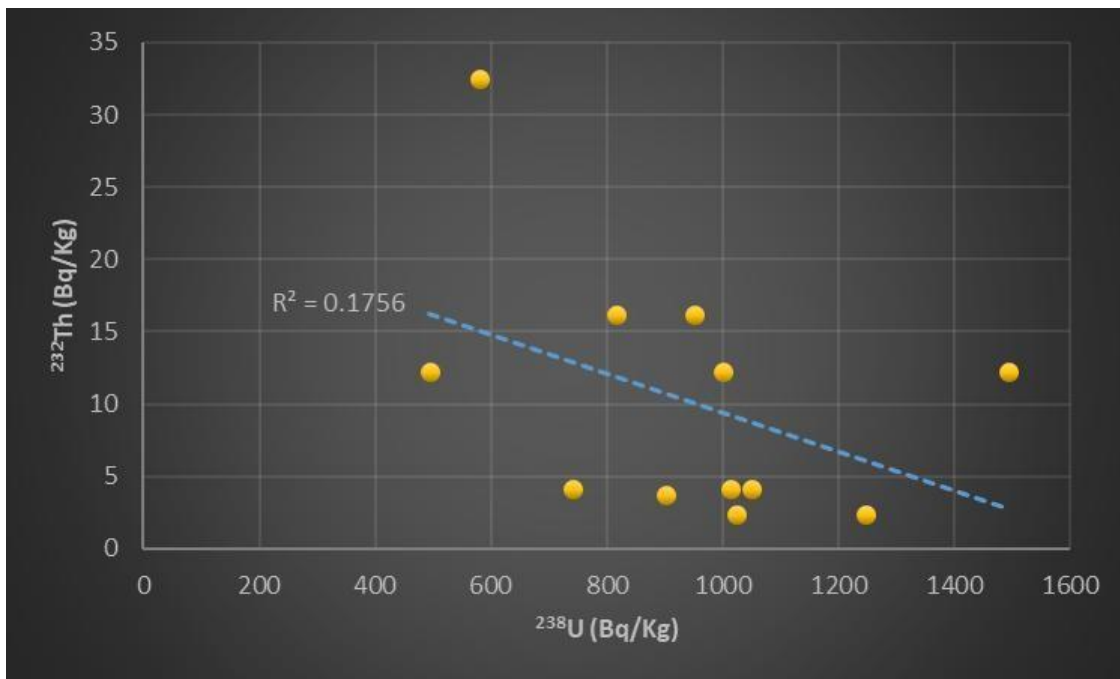


Fig.6Correlation analysis between uranium concentration and thorium activity concentration.

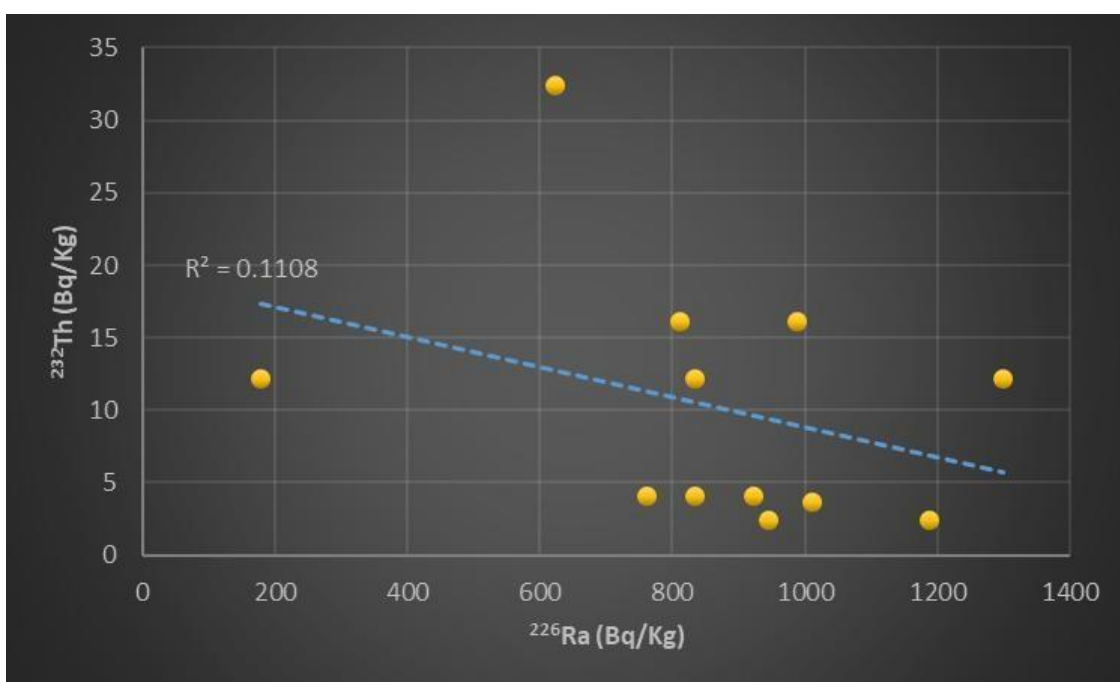


Fig.7 Correlation analysis between radium and thorium activity concentration.

As presented in Table (6), absorbed dose rate in air for each all samples range between 275.5 W to 547.5 M nGy/h, with average 451.75 nGy/h(UNSCEAR 2000 and 2008), so all the samples values of the absorbed dose rates in air are greater than the world average. The effective dose rate equivalent, as show in table (6) are estimated for phosphate rocks samples that ranged between 0.19 at M to 0.38 W ($\mu\text{Sv/h}$) with average 0.32 ($\mu\text{Sv/h}$). The average worldwide was 10 ($\mu\text{Sv/h}$) so all samples values of the effective dose rate equivalent in air are less than the world average limit. The annual effective dose equivalent external (AEDE_{Ex}) for occupational as in table (6), fig. (9), represent the mean value was 1 mSv/y with difference level from 0.61 W to 1.2 M (mSv/y). These values are comparable with the worldwide limit of the occupational that is 20 (mSv/y)(UNSCEAR,2008).

Excess lifetime cancer risk, values are declare in table (6). And fig. (9), ELCR for occupational

has been ranged between the 1 (W) to 1.98 (M) with the mean value of 1.64 mSv/y. These values are greater than a limit of 0.3 the average of worldwide. Alpha index (I_{α}), The values are shown in table (6). Alpha index has a range between the 2 (W) to 5.7 (M) with the mean value of 4.3 (mSv/y). These values are more than unity a worldwide limit average. Annual gonadal dose equivalent. The mean value is 2792.2 ($\mu\text{Sv/y}$). with ranges of data between 1431.8 W to 3633.5 M ($\mu\text{Sv/y}$) as in table (6). All values in five locations were less than the worldwide limit that 300.000 ($\mu\text{Sv/y}$)(UNSCEAR,2008).

Table 6. The calculated hazard parameters of the investigated phosphorite samples.

Locality	S.NO.	Raeq	Hex	Hin	$I_{\gamma x}$	ADRA (nGy/h)	EDRE _{outdoor} ($\mu\text{Sv/h}$)	AEDE _{Ex} (mSv/y)	ELCR (mSv/y)	Alpha index (I_{α})	AGDE ($\mu\text{Sv/y}$)
Hamrawen	H1	868.0	2.35	4.60	5.8	479.31	0.336	1.058	1.74	4.16	2697.0
	H2	786.4	2.13	4.18	5.3	355.76	0.249	0.785	1.29	3.80	2449.0
	average	827.2	2.2	4.4	5.6	417.5	0.3	0.9	1.5	4.0	2573.0
El-Mashash	M3	1022.7	2.76	5.43	6.8	392.65	0.275	0.867	1.42	4.94	3167.7
	M4	1324.8	3.58	7.09	8.9	702.45	0.492	1.551	2.54	6.49	4099.3
	average	1173.7	3.2	6.3	7.9	547.5	0.38	1.2	1.98	5.7	3633.5
Um Hegara	Um5	1051.1	2.84	5.57	7.1	438.07	0.307	0.967	1.59	5.05	3282.1
	Um6	1205.6	3.26	6.47	8.1	585.58	0.410	1.293	2.12	5.94	3739.1
	Um7	964.3	2.61	5.16	6.5	484.44	0.339	1.069	1.75	4.72	2996.4
	average	1073.7	2.9	5.7	7.2	502.7	0.35	1.1	1.8	5.2	3339.2
El-Mashroaa	E8	844.1	2.28	4.47	5.7	454.89	0.318	1.004	1.65	4.05	2615.0
	E9	855.4	2.31	4.56	5.7	496.70	0.348	1.096	1.80	4.16	2659.2
	E10	945.4	2.56	5.05	6.3	480.24	0.336	1.060	1.74	4.61	2938.5
	average	881.7	2.4	4.8	5.9	477.3	0.3	1.1	1.7	4.38	2798.8
West Nile	W11	696.7	1.88	3.56	4.7	303.32	0.212	0.670	1.10	3.11	2173.5
	W12	217.2	0.59	1.07	1.5	247.59	0.173	0.547	0.90	0.89	690.1
	average	457.0	1.2	2.3	3.1	275.5	0.19	0.61	1.0	2.0	1431.8
Max		1173.7	3.2	6.3	7.9	547.5	0.38	1.2	1.98	5.7	3633.5
Min		457.0	1.2	2.3	3.1	275.5	0.19	0.61	1.00	2	1431.8
Total average		898.5	2.4	4.8	6.1	451.75	0.32	1.00	1.64	4.3	2792.2
World limits		370	≤ 1	≤ 1	≤ 1	-	10	20	0.3	≤ 1	300000

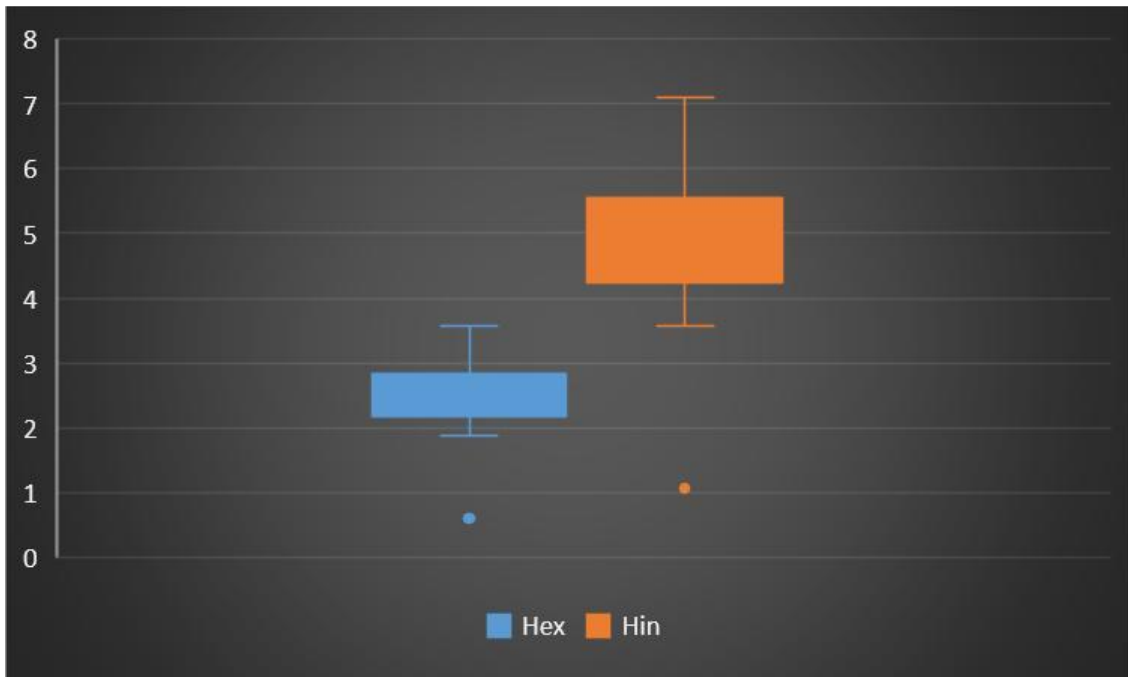


Fig. 8 The correlation between external and internal hazards indices.

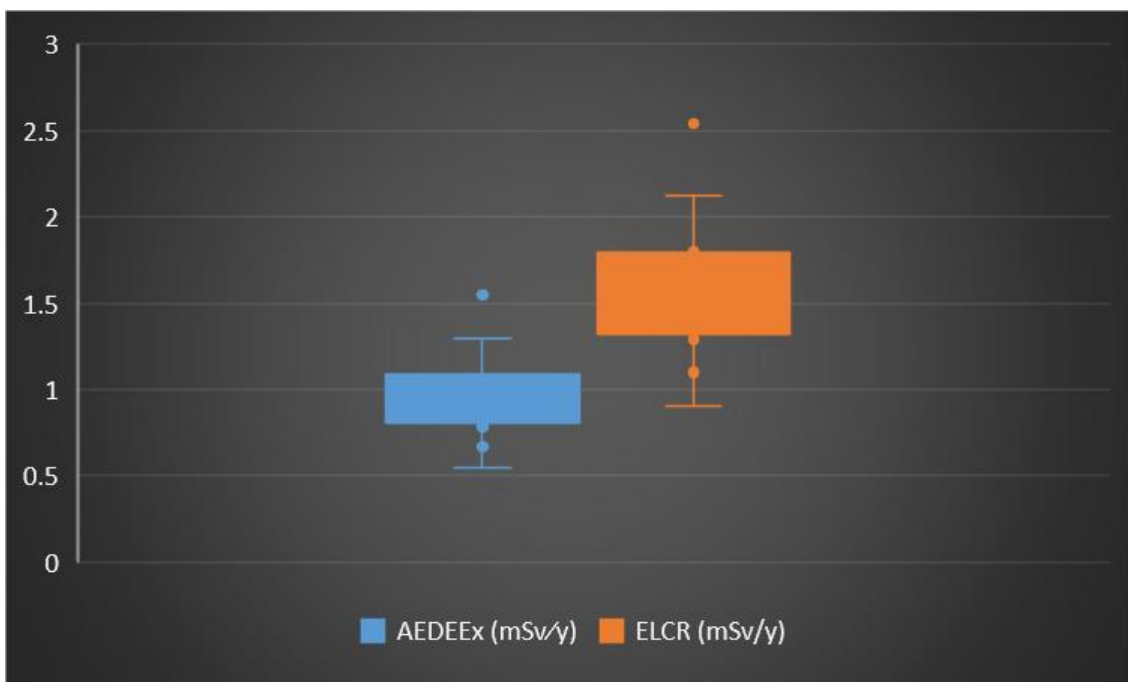


Fig.9 The correlation between the AEDE_{Ex} and ELCR indices.

From the hazard parameters calculated (Table. 6) it is clear that the radium equivalent activity, the external hazard index, the internal hazard index, the representative gamma index, an absorbed dose rate in air (ADRA), the excess lifetime cancer risk (ELCR) and the alpha index (I_{α}) recorded values in all the studied phosphate localities more than the world safe limits.

however, the parameters external exposure, the outdoor effective dose rate equivalent (EDRE), the external annual effective dose equivalent (AEDE_{Ex}) and the annual gonadal dose equivalent [AGDE]) showed lesser values than the world recommended limits.

Table 7. Statistical analysis of an activity concentration of U-238, Ra-226, Th-232, and K-40 *

parameters	Min	Max	Average	W.A
²³⁸ U- (Bq/kg)	537.2	1154.7	942.7	33
²²⁶ Ra- (Bq/kg)	177.6	1143.3	865.3	32
²³² Th-(Bq/kg)	2.9	22.3	10.2	45
⁴⁰ K-(Bq/kg)	131.5	330.2	241.3	412
Ra _{eq} -(Bq/kg)	457	1173.7	898.5	370
H _{in}	1.2	3.2	2.4	≤ 1
H _{ex}	2.3	6.3	4.8	≤ 1
I _γ	3.1	7.9	6.1	≤ 1
ADRA (nGy/hr)	275.5	547.5	451.75	-
EDRE _{outdoor} (μSv/hr)	0.19	0.38	0.32	10
AEDE _{Ex} (mSv/y)	0.61	1.2	1	20
(ELCR) (mSv/y)	1	1.98	1.64	0.3
Alpha index (I _α)	2	5.7	4.3	≤ 1
(AGDE) (μSv/y)	1431.8	3633.5	2792.2	300000

* Parameters abbreviation: radium equivalent (Bq/kg), external and internal index hazard, external level gamma index, absorbed dose rate in air (ADRA), effective dose rate equivalent (μSv/hr), annual effective dose equivalent, excess lifetime cancer risk, Alpha index, Annual gonadal dose equivalent.

From Table 7, its noticed that an average of the activity concentrations of uranium and radium had been exceeded the worldwide average in all five locations with higher values in El-Mashash and the lower values were in the West Nile, nevertheless it's not exceeded the limits for thorium and potassium. And that for Radium equivalent, external, internal hazards indices and representative gamma index all locations exceeded the worldwide average with higher average values in El-Mashash and the lower values in West Nile and for the effective dose rate equivalent external, the annual effective dose equivalent and the Annual gonadal dose equivalent (AGDE) all data were within the limits in five locations and for excess life cancer and alpha index all data was exceeded the limits in all five locations with the highest average values at El-Mashash and the lowest values at West Nile

V. Conclusion.

From the conducted data and the accompanied illustration some conclusions can be formulated as the following, all the selected materials showed the radionuclide activity concentrations more than a range of the average values of worldwide for uranium and radium and less than the worldwide average for both thorium and potassium. Based on the results of radionuclide, the radiological hazards of the radium equivalent activities (Ra_{eq}), external and internal indexes, according to the calculating of absorbed dose rate in air the annual effective dose rate equivalent and AGDE were within the world limits, rather than the Excess life cancer time for workers and alpha index were exceed the safety limits in all five locations.

As a result it's concluded that the variation in these data for some parameter that exceed the safe limits it should be implied that the utilize of that materials should be under control of radiation protection. There is a real probability for undesired radioactive exposure could be received by the workers in the mining facilities in all the studied phosphate localities particularly for those workers who spend long time in the mining activity. The radioactive hazards do not only relate to the gamma emissions but also other risky source represented in the dust

inhalation where the fine particles of the phosphate material containing the radionuclides which come in direct contact with the internal organs and tissues and hence, the alpha particles can cause severe damage for the biological cells. More attention should be delivered for applications of all the proper safety requirements as well as decreasing the working hours for the working-shifts in addition to the periodical medical checkup for the workers. Finally, the obtained data represent the radioactivity background levels in the studied phosphorite localities and could be taken as a reference information to assessment any changes in the radioactivity background level due to the different geological processes in aninvestigated areas.

References

- [1]. Asaduzzaman, K., Mannan, F., Khandaker, M.U.,(2015). Assessment of Natural Radioactivity Levels and Potential Radiological Risks of Common Building Materials Used in Bangladeshi Dwellings, pp. 1–16. <https://doi.org/10.1371/journal.pone.0140667>.
- [2]. Paschoa, A.S., Godoy, J.M.,(2002). The high natural radioactivity and TENORM wastes. In: International Congress Series I225. High Levels of Natural Radiation and Radon Areas. Elsevier Science, Amsterdam, pp. 3–8.
- [3]. El Zrelli, R., Rabaoui, L., Beek, P. Van, Castet, S., Souhaut, M., Grégoire, M., Courjault-rad´e, P., (2019). Natural Radioactivity and Radiation Hazard Assessment of Industrial Wastes from the Coastal Phosphate Treatment Plants of Gabes(Tunisia, Southern Mediterranean Sea), vol. 146, pp. 454–461. <https://doi.org/10.1016/j.marpolbul.2019.06.075>.
- [4]. UNSCEAR (2008). (United Nations Scientific Committee on the Effects of Atomic Radiation), Sources and effects of ionizing radiation. Report to the General Assembly, with Scientific Annexes, UNSCEAR, New York, 2008.
- [5]. Farhan, N., Ridha, A.A., Dheyaa, M., Hanfi, M.Y., Mostafa, M.Y.A., (2021). Materials Today: proceedings Development of alpha tracks measurement with thermal oven as an etching technique for SSNTDs. Mater. Today: Proceedings. <https://doi.org/10.1016/j.matpr.2020.12.232>.
- [6]. Notholt A. J. G. (1985): Phosphoriteresources in the Mediterranean (Tethyan) phosphatic province: a progress report. Sci. Geol. Mem. v.77, p.9-21.
- [7]. Hermina M. H. (1972): Review on the phosphate deposits of Egypt. 2nd Arab. Conf. Mine, Res. Conf. Paper, p.109-149.
- [8]. Khalil M., and Denchi M. L. (2000).Basins geometry and tectonic origin of the western Desert of Egypt, relevance to economic resources. In: El Sayed A.A., Youssef (Eds.), Proceedings of the 5th International Conference on the Geology of the Arab World, Cairo University II, pp. 523–542.
- [9]. Germann K., Bock W. D. Ganz H., SchroterT. and Troger U. (1987). Depositional conditions of Late Cretaceous phosphorites and black shales in Egypt – berl. Geowiss. Abh, (A), Berlin. 75, p.629-668.
- [10]. Glenn C. R. and Arthur M. A. (1990). Anatomy and origin of a Cretaceous phosphorite-green sand giant, Egypt. Sedimentology, v.37, p.123-154.
- [11]. Farai, I.P., Ademola, J.A. (2005) Radium equivalent activity concentrations in concrete building blocks in eight Cities in Southwestern Nigeria. J Environ Radioact 79:119–125.
- [12]. Loucks DP, van Beek E (2017). An introduction to probability statistics and uncertainty water resource systems planning and management. Springer, Cham.
- [13]. Ravisankar, R., Vanasundari, K., Chandra sekaran, A.M., Suganya,P., Vijayagopal, V., (2012). Measurement of Natural radioactivity in building materials of Namakkal, Tamilnadu, India using gamma ray spectrometry. Appl. Radiat. Isotop. 70, 699–704.
- [14]. UNSCEAR (2000). Sources and effects of ionizing radiation. United Nations Scientific Committee on the Effects of Atomic Radiation Sources to the General Assembly with Annexes, Effects and Risks of Ionizing Radiation, United Nations Publications, New York.
- [15]. NEA-OECD, (1979). Exposure to Radiation from Natural Radioactivity in Building Materials. Report by NEA Group of Experts of the Nuclear Energy Agency, OECD, Paris, France.
- [16]. Hazou, E., Patchali, T.E., (2021). Case Studies in Chemical and Environmental Engineering Assessment of radiological hazards in the phosphate mining area of Kpogame, Togo. Case Studies in Chemical and Environmental Engineering 3, 100077. <https://doi.org/10.1016/j.cscee.2020.100077>.
- [17]. Khandaker, U.M., Asaduzzaman, K., Bin Sulaiman, A.F., Bradley, D.A., Isinkaya, M.O., (2018). Elevated concentrations of naturally occurring radionuclides in heavy mineral-rich beach sands of Langkawi Island, Malaysia.Mar.Pollut.Bull.127,654-663.<https://doi.org/j.marpolbul.2017.12.055>.
- [18]. Abdullah, A., (2010). The effect of grain size on the measurements of activity concentration of naturally occurring radioactive materials. Department of Phy., Faculty of Engineering and Physical Sciences, University of Surrey (MPhil to PhM Transfer Report).
- [19]. Ebaid, Y.Y., Bakr, W.F. (2012). Investigating the effect of using granite and marble as a building material on the radiation exposure of humans vol. 151, pp. 556–563.
- [20]. Abo-Elmagd, M., Soliman. H.A., Salman KhA, El-Masry NM (2010). Radiological hazards of TENORM in the wasted petroleum pipes.J Environ Radioact, V 101:51–54.
- [21]. UNSCEAR(1993). Sources Effects and Risks of Ionizing Radiation, Report to the General Assembly, With Annexes, United Nations Scientific Committee on the Effects of Atomic Radiation, United Nations, New York.
- [22]. Abdel-Razek, Y.A., Masoud, M.S., Hanfi, M.Y., El-Nagdy, M.S.,(2016). Science Direct effective radiation doses from natural sources at seila area southeastern desert, Egypt. Journal of Taibah University for Science 10, 271–280. <https://doi.org/10.1016/j.jtusci.2015.06.010>.
- [23]. Ghanim,E.H., Salman, A., Harb,S. (2019). " Radiological risk assessment of phosphate mining in El-Sebaiya locality, Aswan zone, Egypt " RAP Conference Proceedings, vol. 4, pp. 78–82.
- [24]. ICRP. (2007). Recommendations of the International Commission on Radiological Protection, vol. 37, ICRP Publication no. 103, ICRP, Ottawa, Canada.
- [25]. Arafa, W., (2004). Specific activity and hazard of granite samples collected from the eastern desert of Egypt. J. Environ. Radioactivity, 75, 315.
- [26]. Msilax et al.,(2016). "Radioactive nuclides in phosphogypsum from the lowveld region of South Africa," South Afr. J. Sci. 112, 2015–102.
- [27]. Isil Aydin, Firat Aydin, Abdurrahman Saydut, E.GulhanBakirdere, CandanHamamci (2010). Hazardous metal geochemistry of sedimentary phosphate rock used for fertilizer (Mazidag, SE Anatolia, Turkey), Microchemical Journal. 96, 247–251.
- [28]. Negm, S. H. (2014). Radioactivity and Geochemical Studies of the Nile Valley Phosphorites, Egypt. Ph. D. Thesis. Minufiya University.

- [29]. Esmat A. Abou El-Anwar, H.S. Mekky, S.H. Abd El Rahim, S.K. Aita (2017). Mineralogical, geochemical characteristics and origin of Late Cretaceous phosphorite in Duwi Formation (Geble Duwi Mine), Red Sea region, Egypt. *Egyptian Journal of Petroleum*. 26, 157–169.
- [30]. Eduardo Ferreira da Silva, Ammar Mlayah, Celso Gomes, Fernando Noronha, Abdelkrim Charef, Cristina Sequeira, Valdemar Esteves, and Raquel Figueiredo Marques (2010). Heavy elements in the phosphorite from Kalaat Khasba mine (North-western Tunisia): Potential implications on the environment and human health. *Journal of Hazardous Materials*. 182 232–245
- [31]. Germann K., Bock W.D., Ganz H., Schroter T., and Troger U., (1987). Depositional conditions of Late Cretaceous phosphorites and black-shales in Egypt, *Berl. Geowiss. Abh. A* 75 (3) (1987) 629–668.
- [32]. El-Kammar A. M., Zayed M. A. and Amer S. A. (1979). Rare earth of the Nile Valley phosphorites, Upper Egypt; *Chem. Geol.*, v.24, p.69-81.
- [33]. IAEA (2003). Guidelines for radioelement mapping using gamma ray spectrometry, Data IAEA, Vienna, 2003 IAEA-TecDoc-1363. ISSN 1011–4289, Vienna.
- [34]. Ravisankar et al., (2012). Ravisankar, R., Vanasundari, K., Chandra sekaran, A.M., Suganya, P., Vijayagopal, V., 2012. Measurement of Natural radioactivity in building materials of Namakkal, Tamilnadu, India using gamma ray spectrometry. *Appl. Radiat. Isotop.* 70, 699–704.